Proc. Natl. Acad. Sci. USA
Vol. 94, pp. 4395–4400, April 1997
Biophysics

Kinetics of force generation by single kinesin molecules activated by laser photolysis of caged ATP

HIDEO HIGUCHI*†, ETSUKO MUTO*, YUICHI INOUE‡, AND TOSHIO YANAGIDA*‡

*Yanagida Biomotron Project, ERATO, JST, 2-4-14 Senba-Higashi, Mino, Osaka, 562 Japan; and ‡Department of Biophysical Engineering and School of Medicine, Osaka University, Toyonaka, Osaka, 560 Japan

Communicated by James A. Spudich, Stanford University, Stanford, CA, February 24, 1997 (received for review July 29, 1996)

ABSTRACT **To relate transients of force by single kinesin molecules with the elementary steps of the ATPase cycle, we measured the time to force generation by kinesin after photorelease of ATP from caged ATP. Kinesin-coated beads were trapped by an infrared laser and brought onto microtubules fixed to a coverslip. Tension was applied to a kinesin-microtubule rigor complex using the optical trap, and ATP was released by flash photolysis of caged ATP with a UV laser. Kinesin started to generate force and move stepwise with a step size of 8 nm at average times of 31, 45, and 79 ms after photorelease of 450, 90, and 18 μM ATP, respectively. The kinetics of force generation were consistent with a two-step reaction: ATP binding, with an apparent second-order rate constant of 0.7 $\mu M^{-1} \cdot s^{-1}$, followed by force generation at 45 s^{-1} per kinesin molecule. The transient rate of force generation was close to the rate of the ATPase cycle in solution, suggesting that the rate-limiting step of ATPase cycle is involved with the force generation.**

Motor proteins, such as kinesin, myosin, dynein, and RNA polymerase, convert the chemical energy of ATP hydrolysis into mechanical work. To investigate the mechanism of energy transduction of motor proteins, the elementary mechanical steps like force generation and sliding should be related to chemical reactions such as ATP binding, and P_i and ADP release. The biochemistry of ATP hydrolysis by kinesin in solution has been investigated using native and recombinant proteins, with or without microtubules. The ATPase rate of kinesin is very low ($<0.01\ s^{-1}$) in the absence of microtubules at room temperature and is activated more than 2,000-fold by microtubules to $>20\ s^{-1}$ (1–5). The intermediate states of the kinesin-microtubule complex are similar to those of actomyosin, that is, M·K, M·K·ATP, M·K·ADP·P_i, and M·K·ADP, where M, K, and P_i are microtubule, kinesin, and inorganic phosphate, respectively. The rate-limiting step of the ATPase cycle is ADP release in the absence of microtubules, and P_i or ADP release in the presence of microtubules (1–5).

These biochemical results cannot be correlated directly to the mechanical cycle of kinesin, because the movements are not detected in solution. A powerful method for the investigation of mechanochemical coupling is to detect the mechanical change after laser photolysis of caged compounds, e.g., caged ATP, caged ADP, and caged P_i (6, 7). Caged compounds photolyze within several milliseconds after a pulse of ultraviolet light. The mechanical reactions of actomyosin in muscle have been detected after release of ATP by photolysis of caged ATP. The rate of actomyosin dissociation after ATP release and rate of force generation were determined (6).

In the experimental systems containing many molecules, individual events are averaged and the state of each molecule is not determined. Analysis of the events produced by single molecules reveals the molecular functions more directly. The kinetics of single ion channels were elucidated by stochastic analysis of their currents (8, 9). Detection of the single-channel current was much easier than that of force and displacement by single-motor protein molecules because a huge number of ions (about 10^6) flow during single-channel openings and energy consumed by the ion flow is about 10^5-fold greater than the free energy (10^{-19} J) liberated by hydrolysis of single ATP molecules that promote the movement of motor proteins. Recent progress in the measurement of force and displacement of single kinesin or myosin molecules provides the opportunity to directly determine their mechanical properties (10–15). The resolution of the measurement system is about 10^{-20} J, which is close to the energy consumed by the flow of single ions through a channel. It was reported kinesin moves by elementary steps of 8 nm on microtubule protofilaments and produces a maximum stall force of several piconewtons (10–12).

Combining the measurement of force produced by single molecules with photolysis of caged compounds, we have observed mechanochemical coupling events in single motor molecules. We measured the force and displacement of single kinesin molecules using laser trapping and nanometry (10) after initiation of the chemical and mechanical reactions by photolysis of caged ATP. Data were analyzed using statistics. The results indicate that kinesin binds ATP with a rate constant of $0.7\ \mu M^{-1} \cdot s^{-1}$ and subsequently produces force with a rate constant of $45\ s^{-1}$ at 26°C.

Preliminary results have been reported (16).

MATERIALS AND METHODS

Apparatus. A microscope was assembled in-house by mounting lasers, lenses, dichroic mirrors, objective lenses, and *xyz*-translation stages on a vibration-free table (1810LA, HERTZ, Kanagawa, Japan) (Fig. 1*a*). The optical trap used a diode pumped, Nd:YAG infrared laser (wavelength = 1,064 nm; MYLS-300-S-OEM, Santa Fe Laser), and an objective lens (Plan NCF Fluor ×100, Nikon). The trapping stiffness ($0.07–0.25\ pN \cdot nm^{-1}$) was determined from thermal fluctuations of trapped beads using the equipartition law (10). Fluorescence images of fluorescently labeled microtubules and kinesin-coated beads, excited by a frequency-doubled Nd:YAG green laser (wavelength = 532 nm; model 140-0534-100, Light Wave Electronics, Mountain View, CA), were recorded by a high-sensitivity silicone-intensified target camera (C2741, Hamamatsu Photonics, Hamamatsu City, Japan) and displayed on a television monitor (17). The transmitted bright-field image of the bead, illuminated by the green laser, was projected onto a quadrant photodiode (s944–13, Hamamatsu Photonics) via an objective lens (Plan ×100,

The publication costs of this article were defrayed in part by page charge payment. This article must therefore be hereby marked "*advertisement*" in accordance with 18 U.S.C. §1734 solely to indicate this fact.

0027-8424/97/944395-6$2.00/0
PNAS is available online at **http://www.pnas.org**.

†To whom reprint requests should be addressed. e-mail: higuchi@yanagida.jst-c.go.jp.

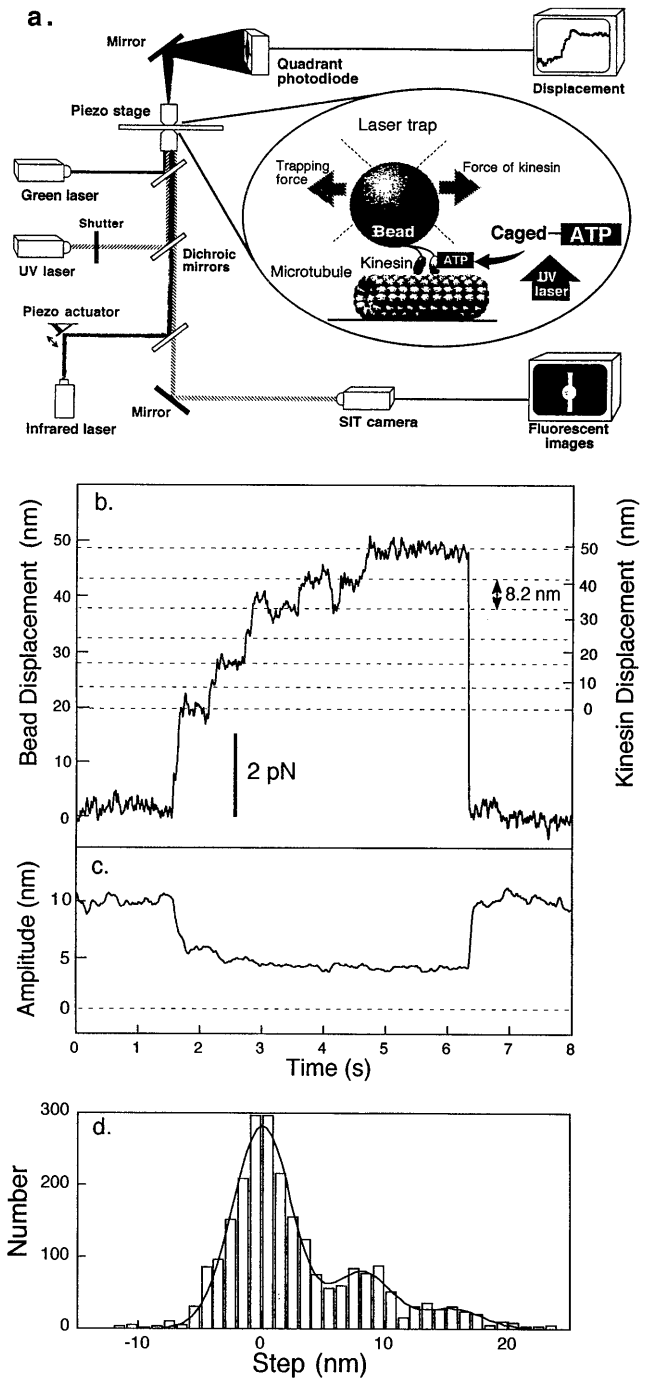

FIG. 1. Measurement of force and displacement of single kinesin molecules. (*a*) Diagram indicating the experimental arrangement for laser trapping nanometry of displacement and force generation by single kinesin molecules activated by flash photolysis of caged ATP. (*b*) Measurement of stepwise movement of a single kinesin molecule at 20 μM ATP. Force was calculated from displacement of the bead multiplied by the trapping stiffness of 0.18 pN·nm^{-1}. The displacement of kinesin, right axis, was determined from the bead displacement, left axis, by correcting for the kinesin-to-bead stiffness shown as follows. (*c*) Determination of kinesin-to-bead stiffness. The amplitude of displacement change of the bead was measured when the center of the trap was sinusoidally vibrated at 500 Hz with a peak-to-peak amplitude of 10 nm. The sinusoidal amplitude decreases when kinesin binds to the microtubule. Kinesin-to-bead stiffness (k_L) was given by the initial peak-to-peak amplitude (10 nm) and the peak-to-peak amplitude (x nm) during force generation as $k_T(10 - x)/x$, where k_T is the trapping stiffness. The kinesin displacement is given by $d_b \cdot [(k_L + k_T)/k_L] = d_b \cdot [10/(10 - x)]$, where d_b is displacement of the bead. (*d*) Histogram of step size. A 100-ms window is moved every 5 ms, and the net displacement of kinesin during the window was measured at 20 μM ATP. The histogram was fitted with the sum of three Gaussian distributions.

Nikon). Displacements of the bead in orthogonal directions were determined from the differential outputs of the quadrant photodiode amplified by a differential amplifier (OP711A, Sentec, Osaka, Japan). Data were filtered by a low pass filter of 4th order Butterworth having a 200-Hz cut-off frequency, and then sampled using a MacLab system (A-D board and data acquisition software; ADInstruments, Australia) at a sampling rate of 1 kHz. To improve detection of step movements, digitized data were passed through a median filter with a 5-ms window.

To measure the stiffness of the bead-to-kinesin linkage, the center of the trap was vibrated sinusoidally at 300–500 Hz with a peak-to-peak amplitude of 10 nm by a piezo actuator (Fig. 1*a*) (NAL5x5x9, Tokin Tokyo). The amplitude of the sinusoidal displacement of the bead was monitored using a Lock-In Amplifier (SR830, Stanford Research, Sunnyvale, CA). In the data used for detection of active bead displacement, the oscillations were reduced to <0.5 nm by the low pass and median filters.

Sample Preparation. Kinesin was purified from bovine brain by microtubule affinity followed by DEAE chromatography (Fractogel DEAE, Merck) and sedimentation (18). Tubulin was prepared from bovine brain and labeled with tetramethylrhodamine (C-1171, Molecular Probes) (19, 20). Microtubules were prepared by copolymerization of fluorescent and nonfluorescent tubulin in a molar ratio of 1 to 20 and stabilized by 40 μM taxol. Kinesin-coated beads were prepared according to the method of Svoboda and colleagues (10, 21) with modifications. The surface of 1.0-μm diameter fluorescent latex beads (final concentration of 5% wt/vol or 140 pM, L5280, Molecular Probes) were coated with casein by incubating in a standard solution [80 mM Pipes, pH 6.8/2 mM $MgCl_2$/1 mM ethylene glycol bis(β-aminoethyl ether)-*N*,*N*,*N*′,*N*′-tetraacetic acid (EGTA)/0.7 mg·ml^{-1} casein] for >30 min on ice. The beads (final concentration, 70 pM) were then rapidly mixed with an equal volume of a standard solution containing kinesin [final concentration, 70–140 pM, assuming a molecular mass of kinesin of 390 kDa (22)], and incubated on ice for >30 min. Fluorescent microtubules (≈10 μg·ml^{-1}) in the standard solution with 10 μM taxol added and no casein were introduced into a flow chamber made of coverslips spaced ≈10 μm apart and allowed to bind directly onto the glass surfaces of a coverslip for 2 min. The remaining surface of a coverslip then was coated with casein by incubation with the standard solution plus 10 μM taxol for 2 min. Finally, the chamber was filled with an assay solution containing the beads and an enzymatic oxygen scavenging system (23) [≈0.1 pM kinesin-coated beads/80 mM Pipes, pH 6.8/2 mM $MgCl_2$/1 mM EGTA/20–500 μM caged ATP [P^3-1-(2-nitrophenyl)ethyl ester of ATP, Dojin]/0.7 mg·ml^{-1} casein/1–25 units·ml^{-1} apyrase (A6535, Sigma)/10 μM taxol/10 mM glucose/0.5% vol/vol 2-mercaptoethanol/50 μg·ml^{-1} glucose oxidase (Sigma G-2133)/9 μg·ml^{-1} catalase (Sigma, C-10), ionic strength ≈50 mM and temperature 25–27°C]. Apyrase was added to scavenge any ATP and ADP contamination in the solution. Concentrations of apyrase were 1, 5, and 25 units·ml^{-1} at 20, 100, and 500 μM caged ATP, respectively. The ATPase activity of apyrase in the assay solution containing ATP was measured by the malachite green method (23). The maximum ATPase activity of apyrase was 6 μM·s^{-1} at 1 unit·ml^{-1} apyrase. Half-saturation of the apyrase activity occurred at 10 μM MgATP.

Photolysis of Caged ATP. For photolysis of caged ATP, solutions containing caged ATP were illuminated by a 5-ms pulse from a continuous wave, near-ultraviolet laser (wavelength = 354 nm, 12 mW; He-Cd 7212I, Liconix, Sunnyvale, CA) equipped with a rapid mechanical shutter (response time

of 0.2 ms, 308B, Cambridge Technology, Cambridge, MA). The trigger for opening the shutter was recorded with MacLab after passing through the 200-Hz low pass filter. The beam of the laser went through an aperture 3 mm in diameter and was focused to a diameter of 30 μm at the surface of the coverslip by the lower objective lens. The energy density of the laser beam at the specimen was 5,400 mW·mm^{-2}, which was calculated from the energy through the objective lens, 3.8 mW, divided by the area of the laser spot, 707 μm^2.

To estimate the fraction of the initial concentration of caged ATP photolyzed by a single laser pulse, the concentration of photoreleased ATP was measured at a known energy density. A chamber made of fused silica glass (path length 2.05 mm) was filled with 90 μl of the assay solution containing 0.215 mM caged ATP. The whole area of the chamber was illuminated by the UV-laser at an energy density of 0.127 mW·mm^{-2} for 1, 2, and 3 s at 25–27°C. The photoreleased ATP was then hydrolyzed by adding 90 μl of a solution containing 0.2 mg·ml^{-1} rabbit skeletal myosin, 200 mM Hepes, 0.6 M KCl, and 20 mM EDTA at pH 7.8 at 25–27°C. After incubation for 10–60 min, the amount of inorganic phosphate (P_i) produced was measured by the malachite green method. Almost all of the photoreleased ATP was hydrolyzed by incubation with myosin within 10 min because the amount of P_i produced was the same after 60 min. The amount of P_i produced per second of illumination was 1.10 ± 0.06% of the total caged ATP (mean ± SD, n = 6). 1.1% photolysis at the energy density of 0.127 mW·mm^{-2} corresponds to 8.7% photolysis per 1 mJ·mm^{-2} of illumination. This value is consistent with that obtained by the photolysis of caged ATP within an 80-μm diameter muscle fiber (7.4% per 1 mJ·mm^{-2}) using a pulsed laser (24). At 5,400 mW·mm^{-2} in the kinesin experiments, the photolysis rate was calculated to be 470 s^{-1} [= ln(1 − 0.011)·5,400/0.127]. For a 5-ms shutter time, the fraction of photolyzed caged ATP is calculated to be 0.90 [= 1 − exp(−0.005·470)].

To calculate the time course of concentration of photoreleased ATP, we determined kinetics of the dark reactions leading to photolysis of caged ATP. Photolysis was simplified to a two-step reaction (25) as follows: The rate of the first step is very high, and the second step (k_c) is rate limiting.

$$\text{Caged ATP} \xrightarrow{\text{fast}} \textit{aci}\text{-nitro intermediate} \xrightarrow{k_c} \text{ATP} + \text{2-nitrosoacetophenone} \quad \textbf{[1]}$$

The rate constant (k_c) was measured by the method of Walker *et al.* (25) with modifications. The assay solution containing 0.5 mM caged ATP was put into a chamber made of fused silica glass. The absorbance of the solution at 405 nm was measured with a mercury arc lamp and a photodiode (Hamamatsu-Photonics, S2545) and amplifier (Sentec OP701A) with a response time of 16 μs. Data were recorded using MacLab software at a sampling rate of 50 kHz. The caged ATP was photolyzed by a 0.3-ms UV pulse (17). The absorbance increased during the UV pulse and then decreased exponentially with a rate constant k_c of 290 s^{-1} at 25–27°C.

The time course for the increase in concentration of ATP was calculated from a rate of photolysis of caged ATP of 470 s^{-1}, k_c of 290 s^{-1}, and a duration of UV flush of 5 ms (Fig. 4, dotted line). The 5-ms flash time was divided into n pieces of short duration, dt. The fraction of caged ATP photolyzed at time of $i{\cdot}dt$ during dt was $[e^{(-470\cdot(i-1)\cdot dt} - e^{(-470\cdot i\cdot dt)}]$, where i is integer and time zero was taken at the time of starting the photolysis,. The fraction of total ATP photoreleased until time t was given by summation from $i = 0$ to $i = t/dt$ at $t < 5$ ms or to n at $t \pm 5$ ms of $[e^{(-470\cdot(i-1)\cdot dt} - e^{(-470\cdot i\cdot dt)}][1 - e^{(-290\cdot t\ -\ i\cdot dt)}]$. The fraction was calculated at dt = 0.5 ms, n = 10 for t = 0 to 200 ms with steps of 1 ms. The ratio of ATP concentration to initial concentration of caged ATP increased to 0.5 at 4 ms, 0.8 at 9 ms, and finally 0.90 at >15 ms (Fig. 4, dotted line). The subsequent decrease due to diffusion of ATP and hydrolysis of ATP by apyrase was neglected. These processes were estimated to be only 5% and 15% of the concentration of the total photoreleased ATP at 100 and 200 ms, respectively, assuming a diffusion constant for ATP of 300 μm^2·s^{-1}, the diameter of photolysis region of 30 μm and the measured ATPase activity of apyrase.

RESULTS

Step Size and Force of Single Kinesin Molecules. The bead sparsely coated with kinesin was put into contact with the microtubule by an infrared laser trap. The position of the bead was determined with nanometer accuracy using a quadrant photodiode (Fig. 1*a*). The kinesin-coated bead moved stepwise in the presence of 20 μM of ATP (Fig. 1*b*). The size of the displacements caused by kinesin were determined accurately from the bead displacements by correcting for the effect of kinesin-to-bead stiffness using a previously described method (13, 26) with modifications (Fig. 1 *b* and *c*). The kinesin-to-bead stiffness was estimated to be 0.17 ± 0.01 pN·nm^{-1} (mean ± SE, n = 31) at a force of 2.5–6 pN. After this correction, the step size of kinesin became about 8 nm, independently of force.

To determine the step size statistically, the difference of displacements between all pairs of data points separated by a time interval of 100 ms was measured and corrected for kinesin-to-bead stiffness (Fig. 1*d*). The position of peaks in histogram was determined to be 0, 8.2, and 15.5 nm by fitting the sum of three Gaussian curves. The step size of 8.2 ± 0.2 nm (mean ± SE) is consistent with the previous values (10, 12) and the spacing of tubulin dimers. The 15.5-nm steps observed are presumably the double steps occurring within 100 ms. The histogram did not show a peak around 5 nm, which was found by Coppin *et al.* (12). The discrepancy may be due to the different substrates, i.e. microtubule (here and ref. 10) or axoneme (12) and bovine (here) or squid (10, 12) kinesin.

To observe the interaction of only one molecule of kinesin with a microtubule, the number of kinesin molecules bound to casein-coated latex beads must be very low. In the present study, 45 beads moved of 112 beads brought into contact with the microtubule at 1 mM steady ATP concentration. Assuming a Poisson distribution of active kinesin molecules on the surface of the beads, the number of kinesin molecules involved in movement of each bead is one, with a probability of > 99% (21). The kinesin-coated beads produced a uniform stall force (6.7 ± 0.2 pN; mean ± SE, n = 36) consistent with previous reports on single kinesin molecules (11, 12, 21). These results demonstrate that single kinesin molecules interact with microtubules in the present conditions.

Force Transient After Photolysis of Caged ATP. Kinesin-coated beads trapped with laser were brought into contact with microtubules attached to a coverslip to form a kinesin-microtubule rigor complex in a solution containing caged ATP (Fig. 1*a*). The rigor complex was stretched by moving the microtubule fixed on the coverslip in the plus end direction by moving the piezo stage (Fig. 1*a*) until the load reached 2.5–5 pN, corresponding to 37–75% of the stall force measured at steady ATP concentrations of 0.02–1 mM. Then, active movement was initiated by photoliberating ATP from caged ATP with a 5-ms pulse of UV-laser light. As described in *Materials and Methods*, the fraction of caged ATP photolyzed was 90%, and the concentration of released ATP was varied by changing the caged ATP concentration. The displacements of kinesin were determined from the bead displacements by correcting for the effect of kinesin-to-bead stiffness (Fig. 1*c*). The stiffness under rigor with caged ATP (0.18 ± 0.01 pN·nm^{-1}, mean ± SE, n = 21) was the same as that during force generation.

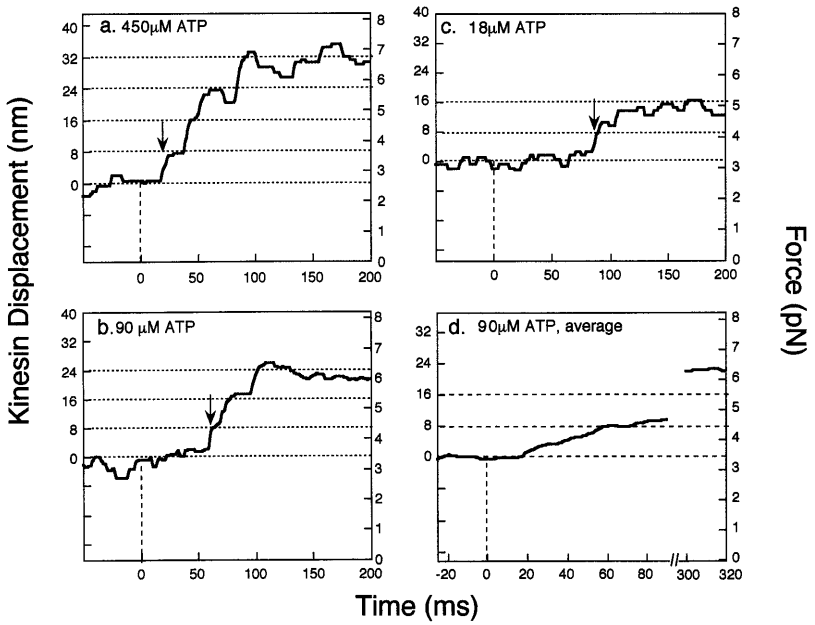

FIG. 2. Displacement and force transients of single or kinesin molecules initiated by flash photolysis of caged ATP at zero time. The initial concentrations of caged ATP were 500 (*a*), 100 (*b*), and 20 μM (*c*), leading to released ATP concentrations of 450, 90, and 18 μM, respectively. The displacements caused by kinesin were determined from the bead displacements by correcting for the effect of kinesin-to-bead stiffness. The arrows in the diagram indicate the moments when the displacements rose to 4 nm above the base lines. (*d*) Fifty-five traces, in which kinesin did not detach from microtubule for at least 350 ms after UV flashes, were averaged. No median filter was used.

Fig. 2 shows the displacement and force transients at released ATP concentrations of 18, 90, and 450 μM. After photolysis of caged ATP (time zero in Fig. 2) and a variable time lag, the beads actively translated in a stepwise manner and then stabilized at a higher force. The size of the steps was ≈8 nm as shown in Fig. 1*b*. The steady force was almost constant at 5–7 pN (Fig. 2), in good agreement with the stalled force measured at steady concentration of ATP.

To detect accurately the time course of force and displacement of kinesin upon ATP binding, displacement noise was reduced by averaging 55 traces of force generation at 90 μM ATP (Fig. 2*d*). No significant change (<1 nm and <0.1 pN) in displacement or force was observed until 15 ms after photolysis. The stalled force at about 300 ms after photolysis was 6.3 pN.

Rate of ATP Binding and Force Generation. The lag time, measured between the caged ATP photolysis and the moment when the displacement reached 4 nm within the first 8-nm step, depended on the concentration of photoreleased ATP (Fig. 2). Fig. 3 shows the distribution of lag times at various photoreleased ATP concentrations. The distributions show peaks at ≈20, ≈30, and ≈70 ms with released ATP concentration of 450, 90, and 18 μM, respectively. The average values of the lag time were 31, 45, and 79 ms at 450, 90, and 18 μM [ATP], respectively.

Fig. 4 shows the time courses of accumulation of kinesin molecules that enter into force generation after photolysis. These populations were obtained by integrating the histograms of the lag times for individual kinesin molecules shown in Fig. 3. The population of force-generating molecules increases sigmoidally (Fig. 4).

After ATP release from caged ATP, the kinetics of entry into force generation can be represented simply as a two-step reaction:

$$\mathrm{M{\cdot}K + ATP} \xrightarrow{k_{ATP}} \mathrm{M{\cdot}K{\cdot}ATP} \xrightarrow{k_f} \text{(Force-generating state)} \quad \textbf{[2]}$$

where K is kinesin, M is microtubule, and k_{ATP} and k_f are rate constants for ATP binding and force generation. The second-order differential equation for the fraction of molecules in a force generating state, [F], is given as (28)

$$d^2[\mathrm{F}]/dt^2 + ([\mathrm{ATP}]{\cdot}k_{ATP} + k_f){\cdot}d[\mathrm{F}]/dt + [\mathrm{ATP}]{\cdot}k_{ATP}{\cdot}k_f[\mathrm{F}] = [\mathrm{ATP}]{\cdot}k_{ATP}{\cdot}k_f[\mathrm{A_o}] \quad \textbf{[3]}$$

where $[\mathrm{A_o}]$ is initial fraction of M·K, that is, $[\mathrm{A_o}] = 1$. The time course of concentration of ATP was shown in Fig. 4 (see *Materials and Methods*). Eq. **3** was solved numerically by computer with MathCAD software (MathSoft, Cambridge, MA) (Fig. 4). The parameters of the best fit are $k_{ATP} = 0.7 \pm 0.2$ $\mu\mathrm{M}^{-1}{\cdot}\mathrm{s}^{-1}$ and $k_f = 45 \pm 10$ s^{-1}. Standard deviations between the fitted curves and data were <2%. The time courses at all three ATP concentrations were well fit with this one set of rate constant.

DISCUSSION

Photolysis of Caged ATP. Recently many caged compounds, such as caged nucleotides (6), caged calcium (29), caged neurotransmitters (30), and caged fluorophores (31) have been synthesized and used to determine the rate of biomolecular chemical or mechanical reactions. In the previous studies, a high power pulsed laser or a xenon flash lamp was used for rapid photolysis of the caged compounds (6, 7, 17). Because the laser beam in this study was focused by an objective lens into a small region, a low-power UV laser (12 mW or 60 μJ per 5-ms pulse) was adequate for photolysis.

Caged ATP is a competitive inhibitor of ATP-driven sliding of actomyosin (ref. 32; H. H. and Y. E. Goldman, unpublished work). Caged ATP also inhibits ATP-driven sliding of kinesin and microtubules in assays of *in vitro* motility. In the conditions used in this study, ATP concentration for half-saturation of kinesin sliding velocity on microtubules was 30 μM, the maximum velocity was 0.95 $\mu\mathrm{m}{\cdot}\mathrm{s}^{-1}$, and the inhibition constant of caged ATP was 120 μM (data were not shown). To avoid the competitive inhibition of movement by caged ATP, most of the

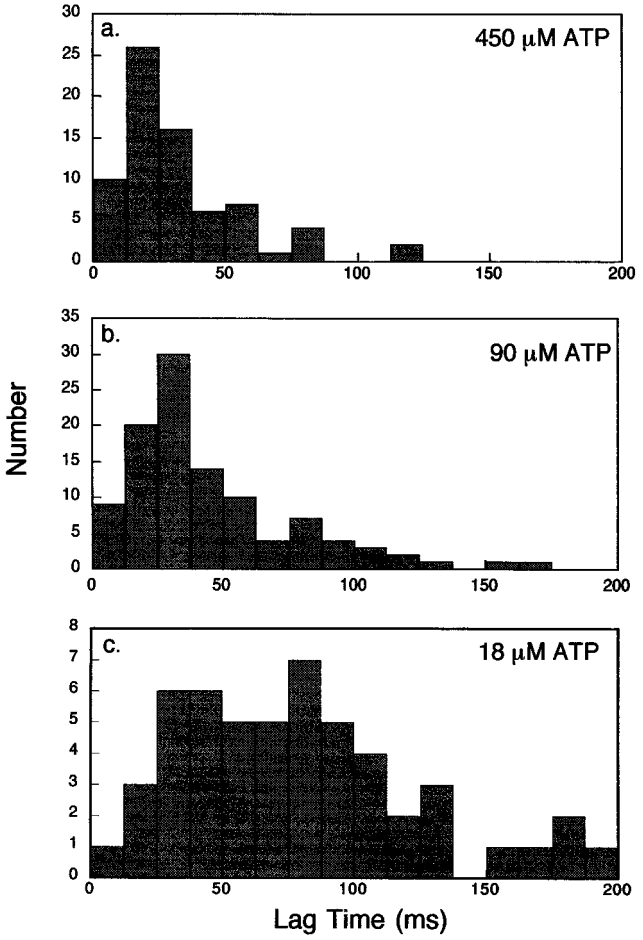

FIG. 3. Histogram of the lag times before displacements occurred. The lag time, measured between the opening of the shutter on the UV laser until the displacement reached 4-nm displacement within the first 8-nm step. The signals of the opening of shutter and the displacement were recorded through 200-Hz low pass filters. Although both signals were retarded by the filter, the lag time was not affected by it. Time bins were 12.5 ms. The final concentration of released ATP was 450 (*a*), 90 (*b*), and 18 μM (*c*).

caged ATP (about 90%) was photolyzed using a continuous wave laser. Under this condition (90% photolyzed and 10% remaining caged ATP), inhibition was negligibly small.

Rigor and ATP Binding State. The binding affinity of kinesin to microtubules in solution, free from load, is high in the absence of MgATP or in the presence of MgAMP-PNP (33, 34). The binding affinity of kinesin to microtubules under a mechanical load had not been measured previously. In the current study, kinesin did not detach from microtubules under 2–5 pN load before photolysis. This indicates that kinesin binds tightly even under load, consistent with results obtained in the presence of AMP-PNP (21). The actomyosin complex in rigor behaves similarly (6).

Until 15 ms after photolysis, no significant change in displacement or force was observed (Fig. 2*d*). At that time, about half of the kinesin molecules should have bound ATP, as calculated from the k_{ATP} = 0.7 $\mu M^{-1}{\cdot}s^{-1}$ and a final ATP concentration of 90 μM. This indicates that ATP binding does not produce a force-generating state according to the two-state model. Even when a large external force was exerted on the bead, kinesin did not promptly dissociate from the microtubule upon photolysis of caged ATP (Fig. 2*d*). The results indicate that the kinesin-ATP complex is tightly bound to the microtubule. This contrasts with the rapid dissociation of the actomyosin complex induced by ATP binding (6).

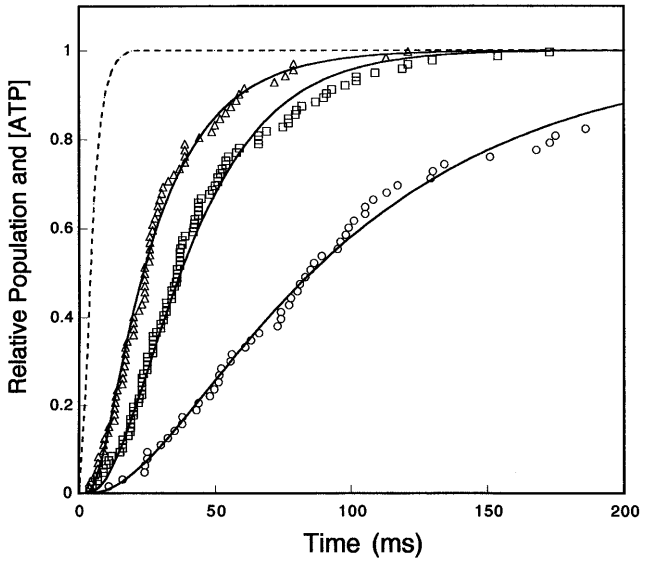

FIG. 4. Kinetic analysis of displacement transients. Dotted line, time course of the increase in ATP concentration after opening of the shutter relative to the final concentration of ATP calculated as described in *Materials and Methods*. Time courses of the accumulation of kinesin molecules in the force-generating state at released ATP concentration of 450 (△), 90 (□), and 18 μM (○). The time courses were obtained by integrating the histograms of the lag times in Fig. 3 using 1-ms time bins. The solid lines are the best fits of the data to a two-step reaction (Eq. **2**, k_{ATP} = 0.7 $\mu M^{-1}{\cdot}s^{-1}$, k_f = 45 s^{-1}) after ATP release from caged ATP. At significance level of 5% in χ^2 test (27), data were fitted to these curves, but not to curves simulated from a model for one-step reaction assuming $k_f \gg k_{ATP}$.

Before photolysis of caged ATP in our experiment, kinesin is bound to the microtubule in the presence of caged ATP. Caged ATP is a competitive inhibitor for motility, suggesting that kinesin binds caged ATP. If photolysis of caged ATP bound to kinesin would lead directly to force generation, then the lag time would have been independent of the concentration of photoreleased ATP. However, the lag time for force development was highly dependent on ATP concentration (Fig. 4), indicating neither that kinesin binds caged ATP nor that heads with bound caged ATP generate the initial force after the flush.

Analysis of the rates of initial force generation at various concentrations of ATP yielded a second order rate constant of 0.5–0.9 $\mu M^{-1}{\cdot}s^{-1}$ for ATP binding to two-headed kinesin molecules bound to microtubules when the external load was 37–75% of the maximum active force. Interpretation of this value in terms of the rate of ATP binding to each head depends on whether the initial force is generated upon ATP binding to either head of the kinesin molecule or only when ATP molecules bind to both heads. In the former case, the rate constant for each head equals the above value, which is approximately half the value (1–3 $\mu M^{-1}{\cdot}s^{-1}$) obtained previously for kinesin bound to microtubules in solution (2, 3). Because the load is expected to be zero in solution, the difference may indicate that the ATP binding rate decreases as the load is increased. If both heads must bind ATP to initiate force generation, then assuming that ATP binds to the heads independently, the rate constant for ATP binding to each head is twice the measured value, i.e. 1.0–1.8 $\mu M^{-1}{\cdot}s^{-1}$. This value is similar to that measured in solution, suggesting that the rate of ATP binding is independent of the load.

Force-Generating State. After ATP binding, a kinesin molecule enters into the force-generating state at the rate of 45 s^{-1}. Block and Svoboda (35) proposed several possible models for stepping movements by kinesin, in which an 8-nm step is generated by the motion of one or two heads. Given the

observed rate of 45 s^{-1}, the rate of force generation for each head of a molecule depends on whether the initial force after the laser flash is generated by motion of either or both heads. In the former case, the rate for each head is 45 s^{-1}. In the latter case, if the two heads behave equally, their individual rates are 90 s^{-1}.

Kinesin ATPase activity is activated more than 2,000-fold by microtubules (1–5). The elementary steps in the ATPase cycle are accelerated by microtubules at 20–25°C from 9 s^{-1} to 100 s^{-1} for ATP hydrolysis (2), from >9 s^{-1} to 20–50 s^{-1} for P_i release (3), and from <0.01 s^{-1} to 40–300 s^{-1} for ADP release (5). If the rate of ATP hydrolysis does not depend on load, the fact that the force-generating rate for each head estimated here (45 or 90 s^{-1}) is smaller than the ATP hydrolysis rate in solution suggests that force is generated after the hydrolysis step. The rate of force generation is close to the ATPase cycling rate of 40–80 s^{-1} per kinesin molecule (20–40 s^{-1} per head) in solution (2–5). Therefore, the rate-limiting step of the ATPase cycle also seems to control the rate of force generation. Discrimination of whether an 8-nm step is generated by one or two heads and whether the ATPase rate depends on the load would allow resolution of the fundamental problem of which biochemical step is involved in the generation of force.

We thank Drs. K. Saito and T. Funatsu for helpful suggestion for building the laser trap apparatus, and Drs. Yale E. Goldman and R. A. Cross for critical reading of this paper.

1. Hackney, D. D. (1988) *Proc. Natl. Acad. Sci. USA* **85,** 6314–6318.
2. Gilbert, S. P. & Johnson K. A. (1994) *Biochemistry* **33,** 1951–1960.
3. Ma, Y. Z. & Taylor, E. W. (1995) *Biochemistry* **34,** 13242–13251.
4. Lockhart, A., Cross, R. A. & McKillop, D. F. A. (1995) *FEBS Lett.* **368,** 531–535.
5. Gilbert, S. P., Webb, M. R., Brune, M. & Johnson, K. A. (1995) *Nature (London)* **373,** 671–676.
6. Goldman, Y. E. (1987) *Annu. Rev. Physiol.* **49,** 637–652.
7. Higuchi, H. & Goldman, Y. E. (1991) *Nature (London)* **352,** 352–354.
8. Kats, B. & Miledi, R. (1972) *J. Physiol. (London)* **224,** 665–699.
9. Neher, E. & Sakmann, B. (1976) *Nature (London)* **260,** 799–802.
10. Svoboda, K., Schmidt, C. F., Schnapp, B. J. & Block, S. M. (1993) *Nature (London)* **365,** 721–727.
11. Meyhöfer, E. & Howard, J. (1995) *Proc. Natl. Acad. Sci. USA* **92,** 574–578.
12. Coppin, Finer, J. T., Spudich, J. A. & Vale, R. D. (1996) *Proc. Natl. Acad. Sci. USA* **93,** 1913–1917.
13. Ishijima, A., Doi, T., Sakurada, T. & Yanagida, T. (1991) *Nature (London)* **352,** 301–306.
14. Ishijima, A., Harada, Y., Kojima, H., Funatsu, T., Higuchi, H. & Yanagida, T. (1995) *Biochem. Biophys. Res. Commun.* **199,** 1057–1063.
15. Finer, J. T., Simmons, R. M. & Spudich, J. A. (1995) *Nature (London)* **368,** 113–119.
16. Higuchi, H., Muto, E., Inoue, Y. & Yanagida, T. (1995) *Jpn. J. Physiol.* **45,** s89.
17. Ishijima, A., Kojima, H., Higuchi, H., Harada, Y., Funatsu, T. & Yanagida, T. (1996) *Biophys J.* **70,** 383–400.
18. Schnapp, B. J. & Reese, T. S. (1989) *Proc. Natl. Acad. Sci. USA* **86,** 1548–1552.
19. Haimo, L. T. & Fenton, R. D. (1988) *Cell Motil. Cytoskelton* **9,** 129–139.
20. Hyman, A. D., Drechsel, D., Kellogg, D., Salser, S., Sawin, K., Steffen, P., Wordeman, L. & Mitchison. T. (1991) *Methods Enzymol.* **196,** 478–485.
21. Svoboda, K. & Block, S. M. (1994) *Cell* **77,** 773–784.
22. Kuznetsov, S. A., Vaisberg, E. A., Shanina, N. A., Magretova, N. N., Chernyak, V. Y. & Gelfand, V. I. (1988) *EMBO* **7,** 353–356.
23. Harada, Y., Sakurada, K., Aoki, T., Thomas, D. D. & Yanagida, T. (1990) *J. Mol. Biol.* **216,** 49–68.
24. Higuchi, H. & Goldman, Y. E. (1995) *Biophys. J.* **69,** 1491–1507.
25. Walker, J. W., Reid, G. P., McCray, J. A. & Trentham, D. R. (1988) *J. Am. Chem. Soc.* **110,** 7170–7177.
26. Kojima, H. Ishijima A. & Yanagida T. (1994) *Proc. Natl. Acad. Sci. USA* **91,** 12962–12966.
27. Kreyszig, E. (1979) *Advanced Engineering Mathematics* (Wiley, New York).
28. Woledge, R. C., Curtin, N. A. & Homsher E. (1985) *Energetic Aspects of Muscle Contraction* (Academic, New York), pp. 119–165.
29. Gurney, A. M., Tsien, R. Y. & Lester, H. A. (1987) *Proc. Natl. Acad. Sci. USA* **84,** 3496–3500.
30. Corrie, J. E. T., DeSantis, A., Katayama, Y., Kjhodakhah, K., Messenger, J. B., Ogden, D. C. & Trentham, D. R. (1993) *J. Physiol.* **465,** 1–8.
31. Mitchison, T. J. (1989) *J. Cell. Biol.* **109,** 637–652.
32. Thirlwell, H, Sleep, J. A. & Frenczi, M. A. (1995) *J. Muscle Res. Cell Motil.* **16,** 131–137.
33. Romberg, L. & Vale, R. D. (1993) *Nature (London)* **361,** 168–170.
34. Crevel, I. M. T. C., Lockhart A. & Cross R. A. (1996) *J. Mol. Biol.* **257,** 66–76.
35. Block, S. M. & Svoboda, K. (1995) *Biophys. J.* **68,** 230s–241s.